Article

Not peer-reviewed version

Impact of Using Flame-Retardant Electrolyte Additives in Li-ion Batteries: A Comprehensive Evaluation of PFPN

Afaque Alam , Samarpan Farmer , Mohammad Behzadnia , Xuefeng Jiao , Brad VanDerWege , Andrew Getsoian , Iyer Claudia , Benjamin Petersen , James Yi , Likun Zhu * , Li Qiao *

Posted Date: 30 April 2026

doi: 10.20944/preprints202604.2175.v1

Keywords: : Li-ion battery; flame-retardant electrolyte additive; PFPN; flammability; thermal stability; thermal runaway

 doi:10.20944/preprints202604.2175.v1

Article

Impact of Using Flame-Retardant Electrolyte Additives in Li-ion Batteries: A Comprehensive Evaluation of PFPN

Afaque Alam [1], Samarpan Farmer [1], Mohammad Behzadnia [2], Xuefeng Jiao [2], Brad VanDerWege [3], Andrew Getsoian [3], Iyer Claudia [3], Benjamin Petersen [3], James Yi [3], Likun, Zhu [2]* and Li Qiao [1]*

[1] School of Aeronautics & Astronautics, Purdue University, West Lafayette, Indiana 47906, USA
[2] School of Mechanical Engineering, Purdue University, West Lafayette, Indiana 47906, USA
[3] Ford Motor Company, Dearborn, MI 48126, USA
* Correspondence: zhu154@purdue.edu (L.Z.); lqiao@purdue.edu (L.Q.)

Abstract

Li-ion batteries (LIBs) are seeing increasingly widespread adoption across consumer electronics, electric vehicles, and grid-scale energy storage systems, yet their susceptibility to thermal runaway remains a concern. This study evaluates ethoxy(pentafluoro)cyclotriphosphazene (PFPN) as an electrolyte additive to improve electrolyte flammability and thermal stability without compromising electrochemical performance. Electrolyte flammability was quantified using Self-Extinguishing Time (SET) measurements, which revealed that PFPN significantly suppresses combustion. At 4 wt% PFPN, 67% of electrolyte samples failed to ignite despite extended ignition exposure, and the average SET decreased by 43% (from 51 s g^{-1} to 29 s g^{-1}). Differential Scanning Calorimetry (DSC) further demonstrated improved thermal stability, with the onset of solvent decomposition delayed by ~30 °C at 4 wt% PFPN. Ionic conductivity modestly decreases (11%, from 10.26 to 9.12 mS cm^{-1} at 4 wt% PFPN). Electrochemical testing showed negligible impact on battery performance. Graphite||Li and NMC811||Li half-cells containing PFPN exhibited comparable capacity retention to baseline cells. NMC811||Graphite pouch cells were used to further evaluate extended cycling and rate capability, PFPN containing cells demonstrated similar capacities even after prolonged cycling and high-rate operation. Overall, PFPN provides effective flame retardance at concentrations as low as 4 wt% while maintaining electrochemical compatibility, making it a promising additive for enhancing thermal stability of LIB electrolytes.

Keywords: Li-ion battery; flame-retardant electrolyte additive; PFPN; flammability; thermal stability; thermal runaway

1. Introduction

The demand for Li-ion batteries (LIBs) has increased exponentially over the past two decades due to its broad application in electric vehicles (EVs), consumer electronics and large-scale energy storage systems. LIBs are the preferred choice for EVs due to their high energy density, long cycle life, low self-discharge, and low environmental impact. LIBs are the central component of EVs which govern the performance, durability, and cost of the vehicle and nearly 41% of malfunctions in EVs are due to Battery failures [1].

As EVs are becoming ubiquitous, the demand for batteries with higher energy density, faster chemical kinetics, and improved thermal management is also growing. An increase in capacity and charging rates is accompanied by greater heat generation, can place greater demands on thermal

 doi:10.20944/preprints202604.2175.v1

management. Sources of heat in LIB can predominantly be classified into two types, namely reversible heat and irreversible heat. Reversible heat generation occurs due to entropy changes and irreversible heat generation in LIBs is due to resistive ohmic losses, overpotential and charge diffusion limitation [2]. In addition, heat generated from the exothermic side reactions exacerbate the condition. If the heat dissipation is insufficient, the temperature of the cell rises resulting in the decomposition of solid electrolyte interphase (SEI) on the anode. This leads to undesired exothermic side reactions between electrolyte and anode material. This further increases the temperature of the cell, initiating a reaction between cathode and electrolyte that leads to the decomposition of cathode material. The exothermic reactions between the cathode and the electrolyte release oxygen and add heat to the cascade reactions that lead to thermal runaway. A comparative study on heat generation from undesired side reactions has been performed by Hou et al. [3]. The contribution of each component in total heat generation was studied by removing one of the three components from the cell and testing the partial cells in an accelerating rate calorimeter (ARC). It was observed that most of the heat generation is due to cathode and anode reaction during the thermal runway event. However, interaction of electrolyte with anode and cathode generates 100% heat at 130.2 °C and 92.6% at 206 °C, respectively. These side reactions serve as the primary trigger for thermal runaway. Consequently, ensuring the stability of electrolyte is crucial for improving LIB thermal stability. At the component level, the most common mitigation strategies involve electrolyte modifications, including the use of solid electrolytes in solid-state batteries, promoting a stable SEI layer, and reducing electrolyte flammability through flame-retardant (FR) additives. The latter has garnered significant attention due to its effectiveness in reducing the flammability of electrolyte with minimal design impact, though it can have adverse effects on the electrochemical performance of the cells. While the direct link between electrolyte flammability and cell-level thermal runaway mitigation remains an active area of research, recent studies have begun to correlate reduced-flammability electrolytes with increased trigger temperatures, lower peak runaway temperatures, and suppressed propagation in pouch and cylindrical cells [4–6]. In the present work, we focus on systematically evaluating the flammability and thermal stability of FR-containing electrolyte, which is expected to contribute to improved battery thermal stability and motivates future cell-level validation studies [4–6].

Phosphorus-containing additives are widely used as flame-retardant for electrolytes due to their effectiveness in reducing flammability and their environmental compatibility. The drawbacks of P-additives are high cost and high viscosity that impact ionic conductivity of the electrolyte [7]. Preventing fire requires inhibiting one of the three essential components of combustion: fuel, oxidizer, and heat [8]. Phosphorus-based additives are known to act primarily by suppressing oxidation reactions at elevated temperatures. They suppress flammability by releasing phosphorus-containing species that interfere with chain-propagating combustion reactions. In addition, certain phosphorus-based additives are known to interact with electrolyte decomposition products such as PF_5, a strong Lewis acid that accelerates solvent degradation, resulting in improved thermal and chemical stability that can be comparatively assessed by DSC. The effects of several P-based additives on the flammability of electrolyte have been studied experimentally in the past. Dagger et al. [9] investigated the effect of several P-based FR additives on flammability and electrochemical stability of the electrolyte (1M LiPF6 in EC: DMC 1:1 wt%). Nitrogen-containing cyclophosphazene additives, particularly PFPN and FPPN, were identified as the most effective in enhancing thermal stability. All tested additives exhibited oxidative stability against a model Pt electrode, although partial electrolyte decomposition was observed during the initial cycles. Li et al. [10] studied the effects of PFPN on flammability and electrochemical performance of LIB cells. The addition of 5% PFPN reduced the SET by 91% and 10% made the electrolyte non-flammable. Interestingly, the addition of PFPN increased the capacity retention and coulombic efficiency by up to 30 cycles. PFPN has also been used to create high capacity 4.6 V cells using LiFSi salt and FEC and PFPN as a solvent. Excellent capacity retention was obtained from the Graphite and NMC811 cells [11].

 doi:10.20944/preprints202604.2175.v1

Most of the past studies with P-additives were done with standard metal oxide cathodes and their compatible electrolytes. New Nickel-rich cathodes offer significantly higher specific capacity of cells, though they are more susceptible to thermal runaway. Thus, a detailed study of P-additives with a compatible electrolyte such as 1M LiPF6 in EC:EMC:DMC with 1% of VC is important for the development of more thermally stable high-capacity LIBs. In the present study, the effectiveness of PFPN in reducing the flammability of electrolyte and its effects on the electrochemical performance was studied.

2. Materials and Methods

2.1. Materials and Sourcing

The baseline electrolyte was a commercial solution of 1.0 M lithium hexafluorophosphate ($LiPF_6$) in a 1:1:1 volume ratio of ethylene carbonate (EC), dimethyl carbonate (DMC), and ethyl methyl carbonate (EMC), containing 1.0% vinyl carbonate (VC) as an additive. The electrolyte was purchased from MTI Corporation (Richmond, CA, USA). The fire-retardant additive evaluated in this study, ethoxy(pentafluoro)cyclotriphosphazene (PFPN, 98% purity), was obtained from BLDpharm (Shanghai, China). PFPN is a phosphorus–nitrogen heterocyclic compound, reported to act as an effective flame suppressant in organic electrolytes.

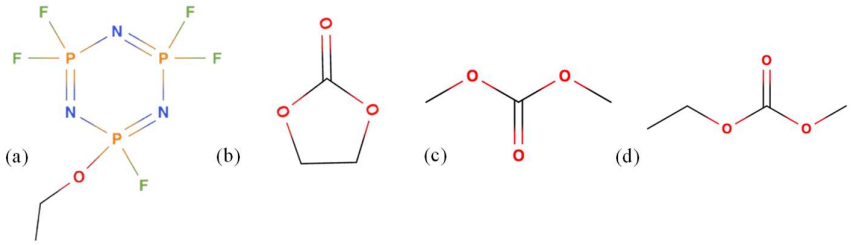

Figure 1. Chemical structures of (a) PFPN and the electrolyte solvents (b) EC (c) DMC (d) EMC.

2.2. Self-Extinguishing Time Test

The Self-Extinguishing Times (SET) test enables us to evaluate an FR additive's performance by measuring the time that an ignited electrolyte sample takes to extinguish itself. A watch glass with a diameter of 6 cm was used to immobilize the electrolyte. A micropipette was used to transfer 400 µL (approximately 0.5g) of electrolyte sample onto the watch glass [12]. The watch glass was placed on a mass balance that recorded the mass of the sample. The test was conducted in an enclosure to eliminate external airflow disturbances, under ambient atmospheric conditions at room temperature. A butane flame torch with a narrow and consistent flame was used to ignite the sample. The ignitor was maintained at a distance such that the ignition flame was not licking the sample or consuming the electrolyte but only providing the ignition temperature [13,14].

Combustion was captured using a high-speed camera; the interval between the removal of the ignition source and the complete extinction of the flame was measured and defined as the burn time. The burn time was normalized against the mass of the sample to give us the SET in s/g.

Ten samples were tested for each PFPN concentration. For the samples that did not ignite within 3 seconds, the exposure to the ignition source was increased progressively to 5 and 8 seconds. The sample was considered ignited only if a sustained flame was observed for at least 5 s.

2.3. Differential Scanning Calorimetry

Differential scanning calorimetry measurements were performed using a TA Instruments DSC Q2000 (TA Instruments, New Castle, DE, USA). Approximately 5 mg of electrolyte was hermetically sealed in gold-plated crucibles designed to withstand pressures up to 300 bar. The samples were

 doi:10.20944/preprints202604.2175.v1

sealed in an Argon filled glovebox and the crucibles were weighed before and after the test to ensure there was no leakage. Nitrogen flowing at 40.0 ml/min was used as the purge gas. The temperature ramp was set to 10.0 °C min^{-1}, since this heating rate provided sufficient resolution to detect any thermal events without introducing noise [15].

2.4. Ionic Conductivity Measurement

The ionic conductivity of the electrolyte was measured using Electrochemical Impedance Spectroscopy (EIS). EIS measurements were performed using a Bio-Logic VSP-300 potentiostat (Bio-Logic Science Instruments, Seyssinet-Pariset, France). An AC voltage of 5 mV was applied over a frequency range of 1 MHz to 1 Hz and the EIS data was collected at six points per decade. The electrolyte was hermetically sealed in the cylindrical volume between two titanium electrodes inside a PTFE Swagelok conductivity cell. The conductivity cells were assembled in an argon-filled glovebox and subsequently transferred to a temperature-controlled chamber, enabling the measurement of ionic conductivity over a temperature range of –40 to 50 °C.

2.5. Electrochemical Performance Tests

Electrochemical cell performance of the electrolyte was tested with created coin half cells and purchased dry pouch cells. Coin-type (2032) half cells were created in an Ar-filled glove box with NMC811 cathode and graphite anode purchased from MTI Corporation. The purchased electrodes were vacuum dried in a vacuum oven for 24 h at 100 °C prior to use, to ensure removal of moisture. Each half cell used Li-metal as the reference electrode and Polypropylene (PP) separator. Each half cell was filled with 40 µL of electrolyte containing varying amount of PFPN. After preparation, the coin cells were allowed to rest at 50 °C for 24 h for wetting the electrodes were charged and discharged at 0.1 C for 2 cycles to promote SEI layer formation. Constant-current charge-discharge tests were carried out using a battery cycler (Arbin instruments). The NMC811 cathode half cells were cycled between the cut-off voltages of 3 V and 4.4 V, and the graphite half cells were cycled between 0.01 V and 1 V. All coin cells were charged and discharged at 0.1 C at room temperature. To test the effect of PFPN containing electrolyte on full cells, 1.1 ml of modified electrolyte was injected in dry pouch cells (LiFun technologies, China) and vacuum sealed the pouch inside a glove box. The capacity of the pouch cells was 0.25 Ah when charged up to 4.4 V. The pouch cells were then rested in an oven at 60 °C for 24 h followed by charging to 3.5 V at 0.04 C and then to 4.1 V at 0.1 C to promote SEI layer formation. The pouch cells were charged and discharged at 0.1 C at room temperature and at 1 C to test extended cycling, between 3 to 4.2 V.

3. Results and Discussion

3.1. Self-Extinguishing Time

The SET test was employed to comparatively assess the flammability of the electrolyte as a function of PFPN concentration. In the absence of PFPN, all baseline electrolyte samples readily ignited with just 3 s of exposure to the ignition source and exhibited sustained combustion, with an average SET of 51 s/g. As shown in Figure 2, with the addition of 1 wt% PFPN, the SET slightly decreased to 49 s/g. At 2 wt% PFPN, the SET dropped by 19% to 41 s/g, and a notable increase in ignition resistance was observed as 40% of the samples failed to ignite. At a concentration of 4 wt% PFPN, the electrolyte exhibits markedly higher ignition resistance. Despite extending the ignition exposure to 5 s, 67% of the samples did not ignite. Among the samples that did ignite, the average SET further decreased to 29 s/g, corresponding to a 43% reduction compared to the baseline.

 doi:10.20944/preprints202604.2175.v1

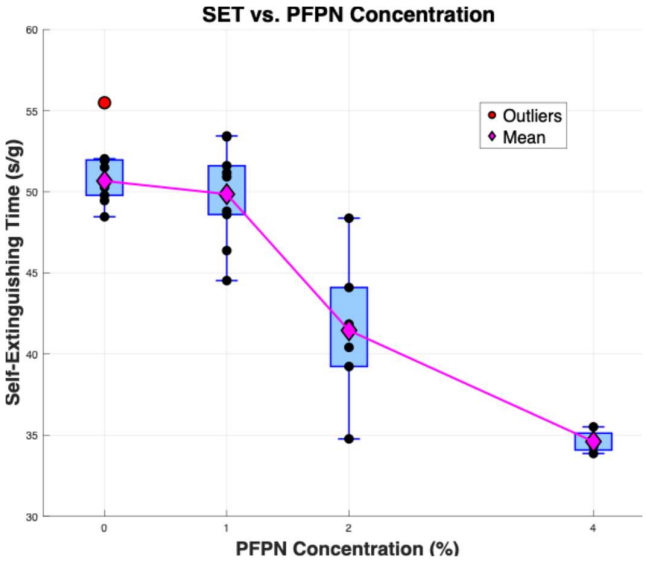

Figure 2. Self-extinguishing Time of Electrolyte with different concentrations of PFPN.

Prior studies of phosphorus- and fluorine-based flame-retardant additives have generally attributed the observed reduction in flame persistence to a combination of radical scavenging, thermal quenching, and dilution effects. Electrolyte combustion is fundamentally driven by radical-mediated reactions; disrupting this radical chain reaction is therefore essential for effective flame suppression [8,16]. PFPN generates phosphorus-based radicals such as PO•, which are known to scavenge H• and OH• radicals and form more stable, less reactive species. Additionally, the fluorine atoms in PFPN release F• radicals, which also bind with H• radicals, preventing them from reacting with O_2 and continuing the combustion process [17].

3.2. Differential Scanning Calorimetry

A DSC test helps identify and isolate the different stages of the thermal decomposition of an electrolyte and determine the inherent thermal stability of an electrolyte. In the DSC test, when an electrolyte sample is subjected to a temperature range, two prominent thermal events are observed (Figure 3). The first is an endothermic peak that corresponds to a phase transition and decomposition of LiPF6, producing PF5 gas [18,19] observed at 250 °C. The second is a highly exothermic decomposition of carbonate solvents (EC, DEC, DMC) via ring-opening and polymerization reactions known to be catalyzed by the PF5 produced by the decomposition of the salt [20]; this peak is observed to start at 270 °C for the baseline electrolyte. Inhibiting or delaying these decomposition reactions could significantly enhance the thermal stability of the battery electrolyte. In a DSC test, this enhancement in thermal stability is demonstrated as a shift in the onset temperature of solvent decomposition. The addition of PFPN shifts both thermal events; it shifts the onset of the thermal decomposition by 21°C with the addition of just 1% PFPN. It further shifts by 7°C with the addition of 2% PFPN, with the addition of 4% PFPN a total shift of 30°C from the baseline electrolyte is observed which marks a significant improvement in the thermal stability.

 doi:10.20944/preprints202604.2175.v1

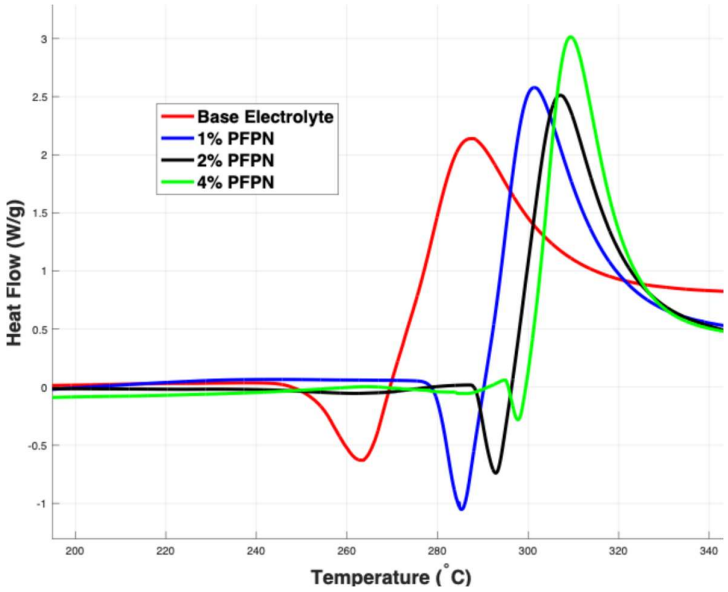

Figure 3. Thermal decomposition characteristics of electrolytes containing varying concentrations of PFPN.

3.3. Ionic Conductivity

Ionic conductivity of the electrolytes was measured using electrochemical impedance spectroscopy (EIS), and the results are summarized in Table 1, which shows the effect of introducing PFPN to the electrolyte. At room temperature, the baseline electrolyte exhibits a conductivity of 10.26 mS/cm, the addition of 4 wt% PFPN reduces it to 9.12 mS/cm, corresponding to an 11% decrease. This decrease is primarily due to the higher viscosity and lower dielectric constant of PFPN, which hinders ion mobility [21–23]. While the incorporation of PFPN results in a marginal drop in ionic conductivity, the values remain within a reasonable range for practical operation.

To examine how conductivity varies with temperature and whether PFPN exerts a similar effect across the entire range, measurements were conducted from –40 °C to 50 °C. As expected, conductivity increased with temperature for all samples. A consistent trend of reduced conductivity with increasing PFPN concentration was observed across the entire range, as seen in Figure 4. These measurements indicate that PFPN only modestly impacts ionic transport, largely because of the low concentrations employed.

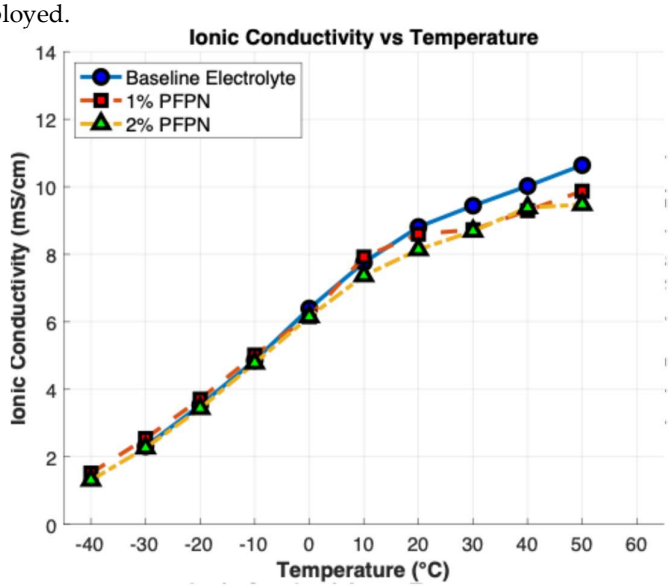

Figure 4. Ionic conductivity of Electrolyte at different temperatures.

 doi:10.20944/preprints202604.2175.v1

Table 1. Ionic Conductivity of Electrolyte at 25°C with different PFPN concentrations.

PFPN Concertation (wt %)	0% PFPN	1% PFPN	2% PFPN	4% PFPN
Ionic Conductivity (mS/cm)	10.26	10.02	9.88	9.12

3.4. Coin cell Cycling

The electrochemical performance of the electrolyte containing varying percentage of PFPN was tested with coin half cells and a 0.25 Ah pouch cell. Cells containing electrolytes with 1% and 2% PFPN additives were compared against a baseline cell containing 0% PFPN. Each coin cell underwent a standard formation process to ensure electrode wetting and SEI layer development, allowing the cells to reach their maximum capacity. These formation cycles were omitted from the data to enable better comparison of cycling performance.

Fig 5(a) and (b) show the results of cycling the anode and cathode half cells with electrolyte containing 0%, 1% and 2% PFPN, at a constant current of 0.1 C rate with upper and lower cut-off voltages of 3 V and 4.4 V for the cathode and 0.01 V and 1 V for the anode half-cells. The initial specific discharge capacity of the anode half-cell was 339.1, 338.8 and 338.2 mAh/g for 0%, 1% and 2% PFPN and it remains nearly constant through the 20 cycles. The secondary axis of plot (a) and (b) in Figure 5 indicates the coulombic efficiencies of the cells. The coulombic efficiencies of the anode half-cell remain stable throughout the cycling process at 99.8% for all three cells.

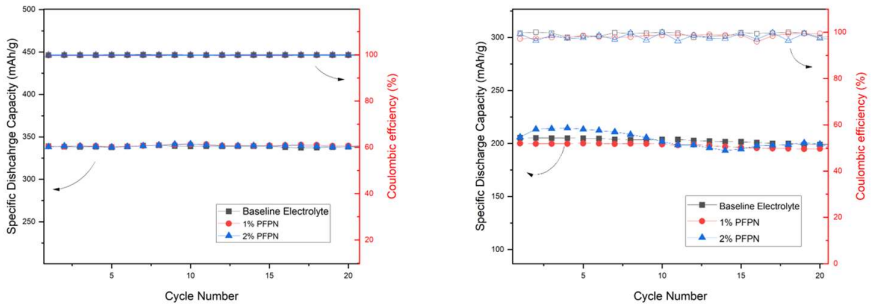

Figure 5. (a) Anode and (b) Cathode Half-cell cycling results.

Figure 5 (b) shows results from the constant current charge-discharge cycling of cathode half-cells at a 0.1 C or 20 cycles. The initial specific discharge capacity of the cathode half-cell was 206.07, 200.2 and 206.07 mAh/g for 0%, 1% and 2% PFPN. After 20 cycles the discharge capacity was 199.32, 195.14 and 199.32 mAh/g for 0%, 1% and 2% PFPN. The coulombic efficiencies of the cathode half-cells during the first charge and discharge cycle were 99.64%, 97.18% and 99.23% for the electrolyte containing 0%, 1% and 2% PFPN and at the 20th cycle the efficiencies were 99.86%, 99.42% and 97.32%. The results highlight that no considerable change in discharge capacity during constant current charge discharge cycling was observed due to the addition of PFPN.

Figure 6 shows the voltage profile during charging and discharging the half coin cells containing 0%, 1% and 2% PFPN additive in the electrolyte. The graphite anode half cells were cycled between 0.01 and 1 V. During the first cycle, the cells with base electrolyte and the cells with electrolyte containing 1% and 2% PFPN were charged to was 339.1, 338.8 and 338.2 mAh/g. The addition of 2% of PFPN to the electrolyte reached marginally higher capacity. Similarly, the discharge capacity was also observed to be very similar, showing that addition of up to 2% PFPN did not degrade the initial capacity of the cells.

 doi:10.20944/preprints202604.2175.v1

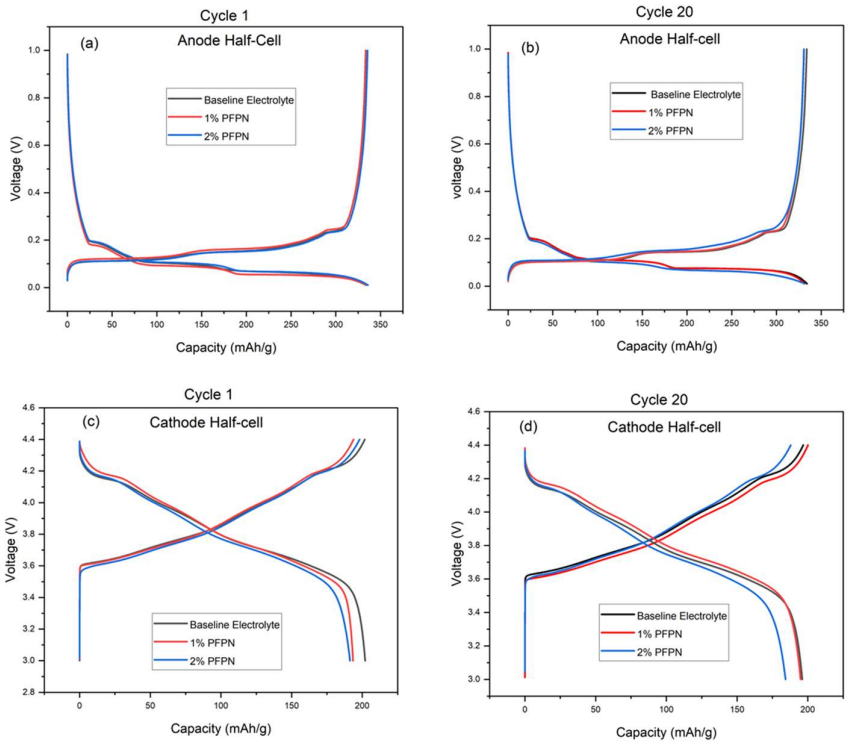

Figure 6. Charge discharge voltage profile of Anode half-cell at (a) 1st and (b) 20th cycle and Cathode half-cell at (c) 1st and (d) 20th cycle.

Figure 6 (c) and (d) show the charge discharge curve of NMC 811 half cells during cycle 1 and 20. The specific charge capacity of the cathode half-cell with base electrolyte reached 202 mAh/g whereas, cells with 1% and 2% PFPN reached 193 and 198 mAh/g. Similarly, the discharge capacity was observed to be 202, 193 and 191 mAh/g for base cell and cells with 1%, and 2% PFPN. The same trend was observed in the charge and discharge capacity of the cells after 20 cycles. The cells containing 0%, 1% and 2% PFPN retained 97%, 100% and 96% of the initial discharge capacity. Thus, the addition of PFPN has no significant impact on the capacity of both cathode and anode half-cells. A small increase in the activation overpotential was observed between 1st and 20th cycles.

3.5. Pouch cell Cycling

The effect of PFPN on discharge capacity and coulombic efficiency of NMC811|| Graphite pouch cell is presented in Fig. 7. Cells with electrolyte containing 0% and 2 % PFPN were cycled at 0.1 C and 1 C. It is evident that the addition of PFPN did not have significant change in capacity up to 50 cycles. Initial capacity of the cell containing 0% PFPN and 2% PFPN were 0.22 and 0.21 Ah, and both retain 100% of their capacity. Similarly, no significant reduction in coulombic efficiency was observed due to addition of flame retardant PFPN in the base electrolyte. The cells were cycled for 500 cycles at a higher rate to compare effects of PFPN on long-term cycle life for the cell. At 1C, the initial capacity of the cell with base electrolyte reached 0.097 Ah which reduced in the first 200 cycles and retained 70% capacity after 500 cycles. The periodic fluctuation in the cell capacity is attributed to the diurnal temperature changes that affect the cell performance. The Cells containing 2% PFPN followed the same trend. The initial capacity of the cell with 2% PFPN reached the capacity of 0.088 Ah which had slower decrease than the base electrolyte to a capacity of 0.063 Ah after 500 cycles, retaining 72% of the initial capacity.

 doi:10.20944/preprints202604.2175.v1

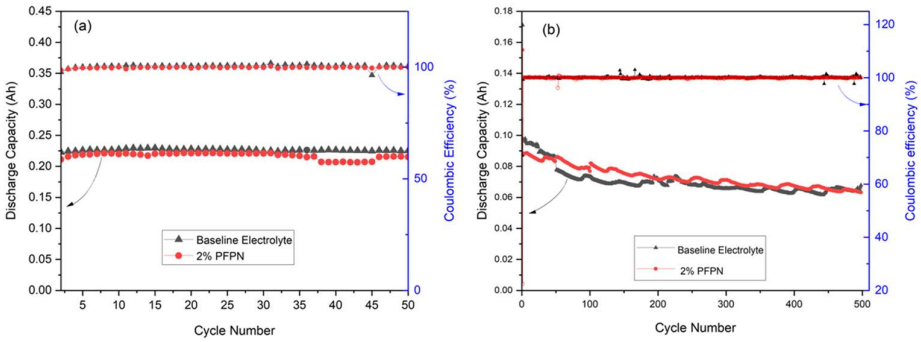

Figure 7. Pouch cell (a) short-term and (b) extended cycling results.

3.6. Rate Capability

The rate performance of full pouch cells, (NMC 811| Graphite) were tested with 0% and 2% PFPN. Both the cells were tested at C-rates ranging from 0.1 C to 2 C and finally again at 0.1 C, between 3 to 4.2 V and the results are compared in Fig. 7. As the C-rate increases, a drop in discharge capacities is observed. The discharge capacities recover back to the initial values, and the C-rate is brought back to 0.1C.

The average discharge capacity of the cell without PFPN is 225 mAh during the initial 5 cycles at 0.1C. For the cell containing 2% PFPN it drops down slightly to 215 mAh. The presence of 2% PFPN is observed to bring about a similar reduction in capacity over the other C-rates. Interestingly this reduction in capacity seems to be less prominent at higher C-rates. Enhanced stability and uniformity of the SEI layer brought about by the presence of PFPN in the electrolyte [23] can suppress the harmful side reactions, maintaining the cyclable lithium content.

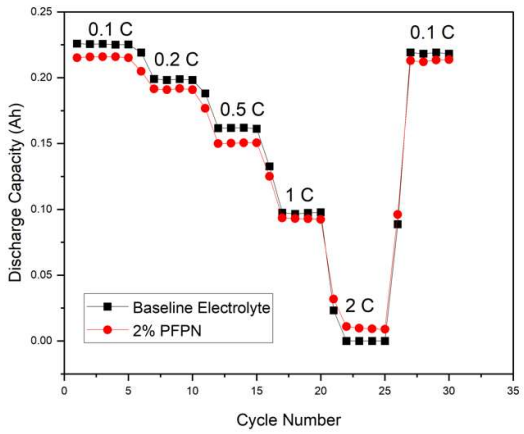

Figure 8. Pouch cell rate capability test results.

4. Conclusions

This work shows that PFPN is a promising electrolyte additive for improving electrolyte flammability resistance and thermal stability, with minimal penalties to Li-ion transport and electrochemical performance. Using the SET measurements, we find that PFPN suppresses ignition and shortens flame persistence: at 2 wt% PFPN, SET drops by ~19% and many samples resist ignition; at 4 wt%, 67% of samples do not ignite even with extended exposure and the average SET decreases by 43% relative to baseline. DSC supports these gains in stability, with the onset of solvent decomposition delayed by up to ~30 °C as PFPN concentration increases to 4 wt%. Ionic conductivity decreases modestly (≈11% at 4 wt%), remaining within a practical range for operation.

 doi:10.20944/preprints202604.2175.v1

Electrochemical testing across graphite||Li and NMC811||Li half-cells, as well as NMC811||graphite pouch cells, indicates that PFPN (≤2 wt%) maintains capacity, coulombic efficiency, and rate capability comparable to the baseline. Short-term cycling shows negligible differences, and extended 1 C cycling to 500 cycles exhibits similar or slightly improved capacity retention with 2 wt% PFPN. Taken together, these trends suggest that low-dose PFPN (≈2 wt%) offers a practical method to improve electrolyte stability in Ni-rich cathode LIBs.

Overall, the results indicate that PFPN effectively improves electrolyte stability while maintaining electrochemical compatibility. The findings highlight the potential of phosphorus–nitrogen flame-retardant additives to enhance the intrinsic thermal stability of next-generation LIBs without compromising performance. While reduced electrolyte flammability and enhanced thermal stability are expected to contribute to improved battery thermal stability, direct validation of these effects on cell-level thermal runaway behavior remains an important topic for future work.

Author Contributions: Conceptualization, L.Q., L.Z., and B.V.; methodology, A.A., S.F., M.B., X.J., L.Q. and L.Z.; validation, A.A., S.F., and M.B.; formal analysis, A.A., S.F., M.B., L.Q., L.Z., B.V., A.G., I.C., B.P., and J.Y.; investigation, A.A., S.F., M.B., L.Q. and L.Z.; resources, L.Q., L.Z., and B.V.; data curation, A.A., S.F., and M.B.,; writing—original draft preparation, A.A. and S.F.; writing—review and editing, L.Q., L.Z., A.G., B.P., J.Y. and B.V.; supervision, L.Q., L.Z., and B.V.; project administration, L.Q., L.Z., and B.V.; funding acquisition, L.Q. and L.Z. All authors have read and agreed to the published version of the manuscript.

Funding: This work was supported by Ford Motor Company.

Data Availability Statement: The raw data supporting the conclusions of this article will be made available by the authors on request.

Acknowledgments: This work was supported by Ford Motor Company.

Conflicts of Interest: Dr. Brad VanDerWege, Dr. Andrew Getsoian, Dr. Iyer Claudia , Dr. Benjamin Petersen, and Dr. James Yi are employed by Ford Motor Company. Other authors declare no conflicts of interest.

References

1. Luo, W., Zhang, S., Gao, Y., and Shen, C., "Review of Mechanisms and Detection Methods of Internal Short Circuits in Lithium-Ion Batteries," *Ionics*, Vol. 31, No. 5, 2025, pp. 3945–3964. https://doi.org/10.1007/S11581-025-06211-6/FIGURES/8
2. Maher, K., Boumaiza, A., and Amin, R., "Understanding the Heat Generation Mechanisms and the Interplay between Joule Heat and Entropy Effects as a Function of State of Charge in Lithium-Ion Batteries," *Journal of Power Sources*, Vol. 623, 2024, p. 235504. https://doi.org/10.1016/J.JPOWSOUR.2024.235504
3. Hou, J., Feng, X., Wang, L., Liu, X., Ohma, A., Lu, L., Ren, D., Huang, W., Li, Y., Yi, M., Wang, Y., Ren, J., Meng, Z., Chu, Z., Xu, G. L., Amine, K., He, X., Wang, H., Nitta, Y., and Ouyang, M., "Unlocking the Self-Supported Thermal Runaway of High-Energy Lithium-Ion Batteries," *Energy Storage Materials*, Vol. 39, 2021, pp. 395–402. https://doi.org/10.1016/J.ENSM.2021.04.035
4. Tran, Y. H. T., An, K., Lim, G., Kim, D., Lee, Y. J., Doh, C., and Song, S. W., "Preventing Thermal Runaway of High-Nickel Li-Ion Battery through Nonflammable Carbonates-Based Electrolyte Formulation," *Materials Science and Engineering: R: Reports*, Vol. 164, 2025, p. 100980. https://doi.org/10.1016/J.MSER.2025.100980
5. Sorensen, A., and Belt, J., "Analyzing Thermal Runaway Propagation in Lithium-Ion Battery Modules with Reduced Flammability Electrolyte Cells," *Journal of The Electrochemical Society*, Vol. 171, No. 8, 2024, p. 080540. https://doi.org/10.1149/1945-7111/AD7293
6. Zhang, W., Feng, X., Huang, W., Lu, L., Wang, H., Wang, L., He, X., Wei, M., Ouyang, M., Zhang, W., Feng, X., Huang, W., Lu, L., Wang, H., Ouyang, M., Wang, L., He, X., and Wei, M., "Thermal Runaway Inhibition of Lithium-Ion Batteries Employing Thermal-Driven Phosphazene Based Electrolytes," *Advanced Functional Materials*, Vol. 35, No. 48, 2025, p. 2508688. https://doi.org/10.1002/ADFM.202508688

 doi:10.20944/preprints202604.2175.v1

7. Dong, L., Deng, L., Wang, Z., Liu, Y., Zhan, J., Wang, S., Fang, Z., Guo, F., Liu, C., Liu, H., and Chen, H., "A Self Fire-Extinguishing and High Rate Lithium-Fluorinated Carbon Battery Realized by Ethoxy (Pentafluoro) Cyclotriphosphazene Electrolyte Additive Design," *Nano Energy*, Vol. 131, 2024, p. 110309. https://doi.org/10.1016/J.NANOEN.2024.110309
8. Kim, J.-H., Hyun, J.-H., Kim, S., Park, H., Yu, S.-H., Kim, J.-H., Hyun, J.-H., Park, W. H., Yu, S.-H., Aiiso, S. K., and Li, Y., "Phosphorus-Based Flame-Retardant Electrolytes for Lithium Batteries," *Advanced Energy Materials*, Vol. 15, No. 23, 2025, p. 2500587. https://doi.org/10.1002/AENM.202500587
9. Dagger, T., Rad, B. R., Schappacher, F. M., and Winter, M., "Comparative Performance Evaluation of Flame Retardant Additives for Lithium Ion Batteries – I. Safety, Chemical and Electrochemical Stabilities," *Energy Technology*, Vol. 6, No. 10, 2018, pp. 2011–2022. https://doi.org/10.1002/ENTE.201800132
10. Li, X., Li, W., Chen, L., Lu, Y., Su, Y., Bao, L., Wang, J., Chen, R., Chen, S., and Wu, F., "Ethoxy (Pentafluoro) Cyclotriphosphazene (PFPN) as a Multi-Functional Flame Retardant Electrolyte Additive for Lithium-Ion Batteries," *Journal of Power Sources*, Vol. 378, 2018, pp. 707–716. https://doi.org/10.1016/J.JPOWSOUR.2017.12.085
11. Chen, L., Nian, Q., Ruan, D., Fan, J., Li, Y., Chen, S., Tan, L., Luo, X., Cui, Z., Cheng, Y., Li, C., and Ren, X., "High-Safety and High-Efficiency Electrolyte Design for 4.6 V-Class Lithium-Ion Batteries with a Non-Solvating Flame-Retardant," *Chemical Science*, Vol. 14, No. 5, 2023, pp. 1184–1193. https://doi.org/10.1039/D2SC05723A
12. Hess, S., Wohlfahrt-Mehrens, M., and Wachtler, M., "Flammability of Li-Ion Battery Electrolytes: Flash Point and Self-Extinguishing Time Measurements," *Journal of The Electrochemical Society*, Vol. 162, No. 2, 2015, pp. A3084–A3097. https://doi.org/10.1149/2.0121502JES/XML
13. Arbizzani, C., Gabrielli, G., and Mastragostino, M., "Thermal Stability and Flammability of Electrolytes for Lithium-Ion Batteries," *Journal of Power Sources*, Vol. 196, No. 10, 2011, pp. 4801–4805. https://doi.org/10.1016/J.JPOWSOUR.2011.01.068
14. Zhang, M., Xiao, J., Tang, W., He, Y., Tan, P., Haranczyk, M., and Wang, D. Y., "A Novel Benchmarking Approach to Assess Fire Safety of Liquid Electrolytes in Lithium-Ion Batteries," *Advanced Energy Materials*, Vol. 14, No. 31, 2024. https://doi.org/10.1002/AENM.202401241
15. Fernandes, Y., Bry, A., and de Persis, S., "Thermal Degradation Analyses of Carbonate Solvents Used in Li-Ion Batteries," *Journal of Power Sources*, Vol. 414, 2019, pp. 250–261. https://doi.org/10.1016/J.JPOWSOUR.2018.12.077
16. Farris, S., Pozzoli, S., Biagioni, P., Duó, L., Mancinelli, S., and Piergiovanni, L., "The Fundamentals of Flame Treatment for the Surface Activation of Polyolefin Polymers – A Review," *Polymer*, Vol. 51, No. 16, 2010, pp. 3591–3605. https://doi.org/10.1016/J.POLYMER.2010.05.036
17. Dong, L., Deng, L., Wang, Z., Liu, Y., Zhan, J., Wang, S., Fang, Z., Guo, F., Liu, C., Liu, H., and Chen, H., "A Self Fire-Extinguishing and High Rate Lithium-Fluorinated Carbon Battery Realized by Ethoxy (Pentafluoro) Cyclotriphosphazene Electrolyte Additive Design," 2024. https://doi.org/10.1016/j.nanoen.2024.110309
18. Zinigrad, E., Larush-Asraf, L., Gnanaraj, J. S., Sprecher, M., and Aurbach, D., "On the Thermal Stability of LiPF6," *Thermochimica Acta*, Vol. 438, Nos. 1–2, 2005, pp. 184–191. https://doi.org/10.1016/J.TCA.2005.09.006
19. Ravdel, B., Abraham, K. M., Gitzendanner, R., DiCarlo, J., Lucht, B., and Campion, C., "Thermal Stability of Lithium-Ion Battery Electrolytes," *Journal of Power Sources*, Vols. 119–121, 2003, pp. 805–810. https://doi.org/10.1016/S0378-7753(03)00257-X
20. Wang, Q., Sun, J., Yao, X., and Chen, C., "Thermal Stability of LiPF6/EC + DEC Electrolyte with Charged Electrodes for Lithium Ion Batteries," *Thermochimica Acta*, Vol. 437, Nos. 1–2, 2005, pp. 12–16. https://doi.org/10.1016/J.TCA.2005.06.010
21. Xia, L., Xia, Y., and Liu, Z., "A Novel Fluorocyclophosphazene as Bifunctional Additive for Safer Lithium-Ion Batteries," *Journal of Power Sources*, Vol. 278, 2015, pp. 190–196. https://doi.org/10.1016/J.JPOWSOUR.2014.11.140
22. Liu, J., Song, X., Zhou, L., Wang, S., Song, W., Liu, W., Long, H., Zhou, L., Wu, H., Feng, C., and Guo, Z., "Fluorinated Phosphazene Derivative – A Promising Electrolyte Additive for High Voltage Lithium Ion

 doi:10.20944/preprints202604.2175.v1

Batteries: From Electrochemical Performance to Corrosion Mechanism," *Nano Energy*, Vol. 46, 2018, pp. 404–414. https://doi.org/10.1016/J.NANOEN.2018.02.029

23. Li, N., Zhang, Y., Zhang, S., Shi, L., Zhang, J. Y., Song, K. M., Li, J. C., and Zeng, F. L., "Insight into the Probability of Ethoxy(Pentafluoro)Cyclotriphosphazene (PFPN) as the Functional Electrolyte Additive in Lithium–Sulfur Batteries," *RSC Advances*, Vol. 14, No. 18, 2024, p. 12754. https://doi.org/10.1039/D3RA08379A